Peer-reviewed version available at Nanomaterials 2018, 8, 738; doi:10.3390/nano8090738

Article

Surface properties of tin dioxide SnO_2 nanowires deposited on Si substrate covered by Au catalyst studies by XPS, TDS and SEM

Monika Kwoka [1]*, Barbara Lyson - Sypien [1] , Anna Kulis [1] , Dario Zappa [2] , Elisabetta Comini [2]

[1] Institute of Electronics, Silesian University of Technology, 44 – 100 Gliwice, Poland; Monika.Kwoka@polsl.pl (M.K.); Barbara.Lyson-Sypien@polsl.pl (B.L.-S.); Anna.Kulis@polsl.pl (A.K.);
[2] SENSOR Lab, Department of Information Engineering (DII), Brescia University, 25123 Brescia, Italy; dario.zappa@unibs.it (D.Z.); elisabetta.comini@unibs.it (E.C.);
* Correspondence: Monika.Kwoka@polsl.pl; Tel.: +48-32-237-2057

Abstract: The surface chemistry and the morphology of SnO_2 nanowires, deposited by Vapour Phase Deposition (VPD) method on Au-covered silicon substrate, were studied before and after subsequent air exposure. For this purpose, surface-sensitive methods including X-ray Photoelectron Spectroscopy (XPS), Thermal Desorption Spectroscopy (TDS) and the Scanning Electron Microscopy (SEM) were applied. The studies presented within this paper allowed to determine the surface non-stoichiometry combined with the presence of carbon contaminations, in a good correlation with the surface morphology. The relative concentrations of the main components [O]/[Sn]; [C]/[Sn]; [Au]/[Sn] together with the O – Sn; O – Si bondings were analyzed. The results of TDS remained in a good agreement with the observations from XPS. Moreover, conclusions obtained for SnO_2 nanostructures deposited with the use of Au catalyst were compared to the previous obtained for Ag-assisted tin dioxide nanowires.

The information obtained within this studies are of great importance for the potential application of SnO_2 nanowires deposited on Au covered Si substrate in the field of novel chemical nanosensor devices, since the results can provide an interpretation of how aging effects influence gas sensor dynamic characteristics.

Keywords: tin dioxide nanowires; surface chemistry; surface morphology; VPD; XPS; SEM, TDS

1. Introduction

Among transparent conductive oxide (TCO) semiconductors applied to the gas sensor devices [1], flat-panel displays [2] and solar cells [3], tin dioxide still remains one of the leading compound under investigation (together with In_2O_3 and ZnO) due to its unique features such as: high electrical conductivity (~ 10^2 Ω^{-1} cm^{-1}) [4], wide band gap (3.6 eV) [5] and transparency in the visible and near infrared region (70–80%).

Recently there is a continuously increasing tendency to fabricate new forms of SnO_2 starting from thick and thin films [6-8] to nano-scale objects such as: nanowires [9-11], nanofibers [12], nanopowders [13] and nanorods [14], with the aim to obtain enhanced and tuned features. In the field of gas sensors, the improved sensitivity, selectivity, thermal stability as well as the speed of response and recovery are the most desired characteristics that can be achieved using nanowires [15,16]. This can be attributed to the high crystallinity, less agglomerated structures' formation as well as the large surface – to – volume ratio. In such structures, about one – third of the atoms are localized just at the surface, where the sensor transduction mechanism takes place, and therefore

leading to the enhancement of the chemical sensing performance (such as catalytic activity or surface adsorption) [17,18].

The development in the field of SnO_2 – based nanowires tends toward intentionally applying not only other metal oxide additives but also noble metal catalysts such as Pd [18-20], Pt [20,21], Ag [9,22] and Au [10,11,23] in order to both induce nucleation of the nanowires [9] and achieve improvement in the sensor signal, operating temperature and stability to humidity [6].

In our previous work [9] we have investigated the surface chemistry of SnO_2 nanowires deposited on Ag – covered Si substrate by Vapor Phase Deposition (VPD) method using the X-ray Photoelectron Spectroscopy (XPS), in combination with Thermal Desorption Spectroscopy (TDS), with the special emphasis on identifying and avoiding carbon contaminations at the surface that are directly related to the aging effects.

Our aim within this work is to present the results of comparative studies of the surface chemistry and morphology of SnO_2 nanowires prepared by VPD method on Au-covered Si substrate after air exposure. Vapor Phase Deposition (VPD) technique is chosen since it is considered as the most successful method for the deposition of SnO_2 nanowires on the Si surface covered with ultrathin layer of metallic catalyst in the form of metallic droplets (metallic seeds), which play a crucial role for the nucleation and growth of SnO_2 nanowires from the gaseous reactants [24]. Moreover, it enables to control the SnO_2 nanowires' size and their density at the substrate [25].

Au – assisted SnO_2 nanostructures exhibit different properties when compared to Pd or Pt – SnO_2 systems (Fermi – level control behavior). As there are reports that neither surface nor bulk interactions take place between Au and SnO_2 [6], the surface chemistry of these nanostructures still needs further investigation and analysis. In order to design a novel gas sensor based on SnO_2 nanowires deposited on Au – coated substrate, which can be treated as the long term perspective for the results of these studies, the knowledge concerning the surface chemistry of this system is crucial.

2. Experimental

2.1. Deposition of SnO_2 nanowires

SnO_2 nanowires were synthesized at SENSOR Lab, Department of Information Engineering (DII), University of Brescia, Italy. The process started from the cleaning of Si(100) wafer in acetone for 15 minutes. After that procedure, the substrate was covered with an ultrathin Au layer (5 nm) deposited by magnetron sputtering (MS) with a RF electrical power of 50 W and 7 sccm Ar flow (Kenotec, Italy). The methodology described above was applied to improve the SnO_2 nanowires nucleation process, since Au metallic seeds act as nucleation sites that promote the growth of SnO_2 nanowires in the Vapor Phase Deposition (VPD) [25].

The deposition of SnO_2 nanowires was performed in a tubular alumina furnace (custom design, based on a Lenton furnace), using SnO_2 powder (Sigma-Aldrich, 99.9% purity) as a source material and heated up to 1370°C in order to start the evaporation process. The mass transport was achieved by introducing an argon flow acting as gas carrier, at the pressure of 100 mbar. After 15 minutes, a dense and homogeneous mat of SnO_2 nanowires have been obtained on the Si substrate covered with Au nanolayers held at the temperature of 900°C.

2.2. Characterization of SnO_2 nanowires

The surface morphology of SnO_2 nanowires (NW) was controlled using a Field Emission Scanning Electron Microscope (FE-SEM, Gemini, Leo 1525). The measurements were carried out at SENSOR Lab at the University of Brescia in Italy. These observations confirmed the nanostructures size and morphology.

In turn, the surface chemistry, including contaminations, of the above mentioned SnO_2 NW was controlled sequentially using XPS in combination with Thermal Desorption Spectroscopy (TDS) method. XPS technique enabled to determine both the surface stoichiometry and contaminations before and after TDS experiments, which allowed us to detect the active gases adsorbed at the surface of SnO_2 NW after air exposure. TDS procedure consisted in measuring gas desorption during the programmable linear growth of the sample temperature (TPD) detected in line by mass spectrometry (MS). These experiments were done at the CESIS Centre, Institute of Electronics, Silesian University of Technology, Gliwice, Poland.

In X-ray photoelectron spectroscopy experiments, the XPS spectrometer (SPECS, Germany) was equipped with a X-ray lamp (AlK_α 1486.6 eV; XR-50 model) and a concentric hemispherical analyzer (PHOIBOS-100 Model). All the reported binding energy (BE) data have been calibrated using the XPS C1s peak (285.0 eV) of residual C contamination at the surface of SnO_2 nanowires. The XPS experiments have been performed at the base background working pressure ~ 10^{-7} Pa.

TDS measurements were performed also at the base background working pressure ~ 10^{-7} Pa in the sample preparation chamber equipped, among other, with the mass spectrometer - residual gas analyzer (Stanford RGA100 Model) and a temperature programmable control unit of OmniVac – Dual Regulated Power Supply PSReg120 model. During every TPD cycle (the temperature increased by 6 °C per minute in the range of 50 - 350°C) the TDS spectra of selected gases like H_2, H_2O, O_2 and CO_2 have been registered.

3. Results and Discussion

Figure 1 presents SEM images of VPD SnO_2 nanowires deposited on Au-covered Si(100) substrate. As it can be seen, the nanowires are isolated, and their length equals to several μm. The diameter, instead, is around 100 nm. Au metallic nanoparticles, which have migrated from the substrate and contributed to the SnO_2 nanowire nucleation process, can be easily identified on the surface of nanostructures.

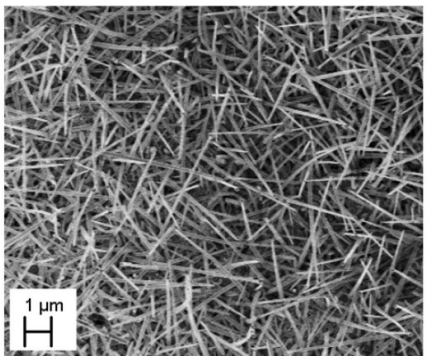

(**a**)

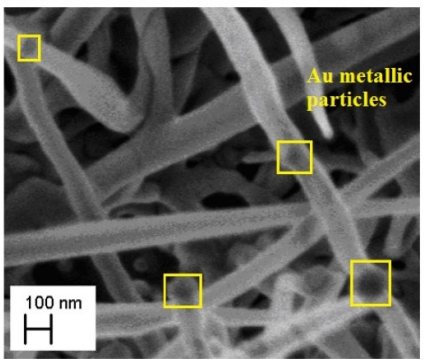

(**b**)

Peer-reviewed version available at Nanomaterials 2018, 8, 738; doi:10.3390/nano8090738

Figure 1. The SEM images (in two scales) of VPD SnO_2 nanowires deposited on Au-covered Si(100) substrate.

Figure 2 shows the XPS survey spectra of the VPD SnO_2 nanowires deposited on Au-covered Si substrate after exposure to air, before and after TPD process.

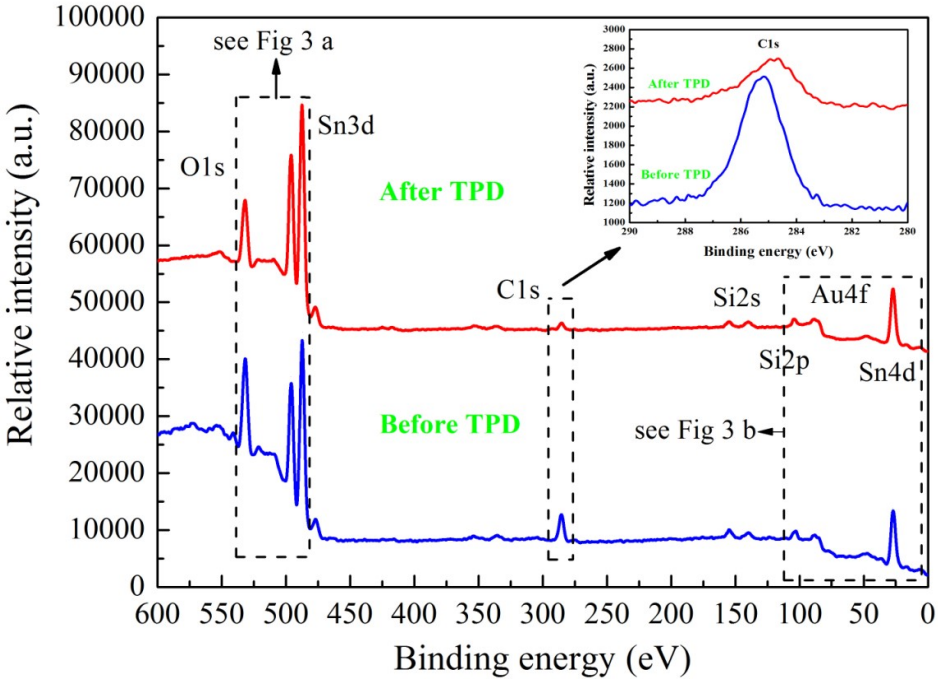

Figure 2. XPS survey spectra with main core level lines of the VPD SnO_2 nanowires deposited on Au-covered Si substrate before and after TPD process.

The spectra contain well-recognized main core XPS levels: O1s, double Sn3d, single C1s and Sn4d peaks, correspondingly labelled. The evident contribution of the XPS C1s peak can be attributed to the carbon contaminations adsorbed at the surface from the air atmosphere. Moreover, the Au4f peaks are present, proving that the metallic Au catalyst appears at the surface of nanowires. This conclusion is opposite to our recent experience, as the presence of Ag catalyst was not observed in VPD SnO_2 nanowires deposited on Ag-covered Si(100) substrate [9].

The inset in **Figure 2** shows in details the binding energy range corresponding to C1s peaks position. As it can be seen, the removal of carbon contaminations during the TDS procedure is not completely possible. Relying on the SEM (**Figure 1**) as well as XPS results before and after TDS procedure (**Figure 2**), it can be concluded that the gold particles can be covered by the carbon and the bonding between them impedes removing C contaminations during the TDS process. This is a limitation that has not been observed in the case of the previously studied Ag - covered Si(100) substrate [9].

The quantitative XPS data analysis was performed to determine the relative concentration of the main components of SnO_2 nanowires under investigation within the escape depth, corresponding to the triple values of inelastic mean free path of photoelectrons.

According to the generally accepted procedure, the relative concentration of the main components can be estimated on the base of the area (intensity) of the main XPS spectral lines within specific spectral windows, acquired with the highest signal to noise ratio (S/N) weighted by the

corresponding atomic sensitivity factor (ASF) [4]. The details of this procedure were already described in reference [4]. **Figure 3** demonstrates the XPS specific spectral windows used for this procedure.

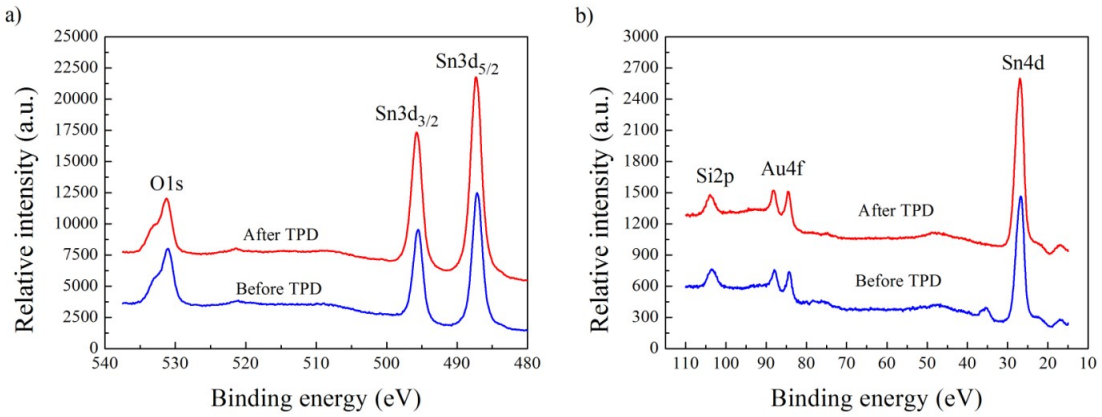

Figure 3. XPS spectral window of: (a) O1s and Sn3d; (b) Si2p, Au4f and Sn4d of the VPD SnO_2 nanowires deposited on Au-covered Si(100) substrate before and after subsequent TDS experiment.

Taking into account the atomic sensitivity factors for respective elements (O1s - 0.711 and $Sn3d_{5/2}$ – 4.725) [26] the relative atomic concentrations [O]/[Sn] were calculated. After the air exposure, the relative [O]/[Sn] concentration at the surface of VPD SnO_2 nanowires deposited at Au-covered Si(100) substrate reached a value of 2.26±0.05. This means that the additional surface oxygen bonding appeared. In turn, after TPD process, the relative [O]/[Sn] concentration decreased to 1.84±0.05. This was in an evident contrary to results obtained for VPD SnO_2 nanowires deposited on Ag-covered Si(100) substrate [9]. Perhaps, it corresponds to the deterioration of their stoichiometry, related to the desorption of weakly (physically) bounded oxygen from the surface of VPD SnO_2 nanowires deposited on Au-covered Si(100) substrate.

Since evident XPS Au4f peaks are observed at the surface of VPD SnO_2 nanowires, both before and after TDS process (**Figure 3b**), the same procedure was applied to determine [Au]/[Sn] ratio. The atomic sensitivity factor for Au4f equals to 6.250 [26]. The relative [Au]/[Sn] concentration before and after TPD process appeared to be constant and equal to 0.11.

Keeping in mind that C contamination at the surface of NWs is crucial, which was confirmed by C1s XPS peaks in the survey spectrum in **Figure 2,** the same procedure was used to determine [C]/[Sn] concentration. The atomic sensitivity factor for C1s is equal to 0.296 [26]. For VPD SnO_2 nanowires deposited on Au-covered Si(100) substrate after air exposure, the relative [C]/[Sn] concentration was estimated as 2.66±0.05, confirming that their surfaces are very strongly contaminated by C species. In turn, after TDS process, the relative [C]/[Sn] concentration decreased more than 5 times, to the value of 0.54±0.05.

The relative concentrations of [O]/[Sn], [C]/[Sn] and [Au]/[Sn] for VPD SnO_2 nanowires deposited on Au-covered Si(100) substrate before and after TDS experiments are summarized in Table 1.

Table 1. The relative concentrations of basic elements for VPD SnO_2 nanowires deposited on Au-covered Si(100) substrate.

Preprints (www.preprints.org) | NOT PEER-REVIEWED | Posted: 27 July 2018 doi:10.20944/preprints201807.0543.v1

Peer-reviewed version available at Nanomaterials 2018, 8, 738; doi:10.3390/nano8090738

Sample status	Relative concentration		
	[O]/[Sn]	[C]/[Sn]	[Au]/[Sn]
Before TPD	2.26 ± 0.05	2.66 ± 0.05	0.11 ± 0.05
After TPD	1.84 ± 0.05	0.54 ± 0.05	0.11 ± 0.05

The variation of relative [O]/[Sn] concentration before and after TDS experiments, summarized in **Table 1,** is in a good correlation with the variation of contribution of respective surface bondings of main elements, observed after the deconvolution of O1s and Sn3d$_{5/2}$ XPS spectral lines (peaks).

In **Figure 4a,c** the XPS Sn3d$_{5/2}$ lines of VPD SnO_2 nanowires before and after TDS are presented. A simple visual shape analysis indicates that they are almost symmetrical. Thus, it is evident that they should contain only the component corresponding to one form of Sn ions.

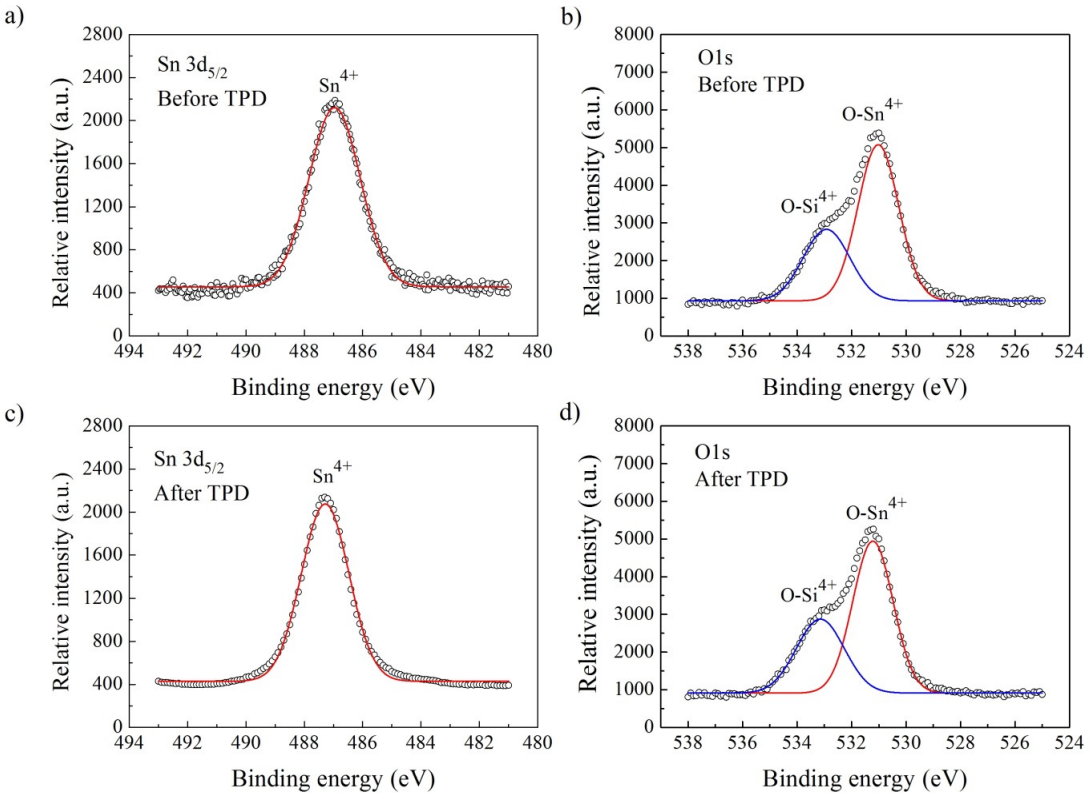

Figure 4. Registered XPS Sn3d$_{5/2}$ and O1s peaks and deconvoluted components of the air exposed VPD SnO_2 nanowires: (a, b) before TDS; (c, d) after TDS process.

The decomposition of Sn3d5/2 peaks allows us to conclude that there is only one contribution observed at the binding energy of 486.6 eV for both Sn3d$_{5/2}$ lines (before and after TDS), corresponding to the Sn^{4+} ions, in a good agreement with NIST database [27]. Therefore, this

confirms that our VPD SnO_2 nanowires consist mainly of tin dioxide SnO_2. This was expected as they have been deposited directly starting from pure SnO_2 powder.

In **Figure 4b,d** XPS O1s lines of air-exposed VPD SnO_2 nanowires are presented. Visual shape analysis indicates that they are evidently asymmetrical, thus they should contain minimum two components corresponding to the various forms of oxygen ions. The decomposition of XPS O1s peaks shows that they are mainly built-up of two contributions observed at the binding energies of: 531.2 eV and 533.0 eV for both samples (before and after TDS procedure).

The first binding energy can be ascribed to the oxygen bondings with the Sn^{4+} ions, whereas the second one to the oxygen bondings with the Si^{4+} ions of the substrate, in a good agreement with NIST database [27]. Therefore, in XPS experiments we have observed a contribution from the Si substrate, meaning that the whole Si substrate surface is not fully covered with VPD SnO_2 nanowires.

The results of the decomposition procedure of XPS $Sn3d_{5/2}$ and O1s peaks obtained for VPD SnO_2 nanowires deposited on Au–covered Si substrate before and after TDS are summarized in **Table 2.**

Table 2. The basic parameters of XPS $Sn3d_{5/2}$ and O1s peaks used in deconvolution procedure and the obtained contribution of main components for the samples before and after TDS

XPS peak parameters	**$Sn3d_{5/2}$**	**O1s**	
Components	**Sn^{4+}**	**O-Sn^{4+}**	**O-Si^{4+}**
Binding energy (eV)	**486.6**	**531.2**	**533.0**
Relative peak area	**1.0**	**0.71**	**0.29**

Based on the information in **Table 2**, only a fraction of measured oxygen is effectively bonded with Sn^{4+} tin. Taking into account the contribution from these O-Sn^{4+} bondings, the real [O]/[Sn] concentration for VPD SnO_2 nanowires before TDS process is smaller than the one obtained from the analysis based on the XPS O1s and $Sn3d_{5/2}$ spectral windows (presented in **Table 1**). It means that these VPD SnO_2 nanowires deposited on Au-covered Si substrate are not fully stoichiometric both before and after TDS.

The fact that the deconvolution procedure leads to the same conclusions for SnO_2 nanowires before and after TDS, means that the surface chemistry of these nanostructures is practically stable. However, the exact value of the relative [O]/[Sn] concentration before and after the TDS process is not clear because of the contribution of the surface contaminations.

All obtained information on the evolution of surface chemistry of VPD SnO_2 nanowires, before and after TPD process, remains in a good correlation with the respective TDS spectra shown in **Figure 5.**

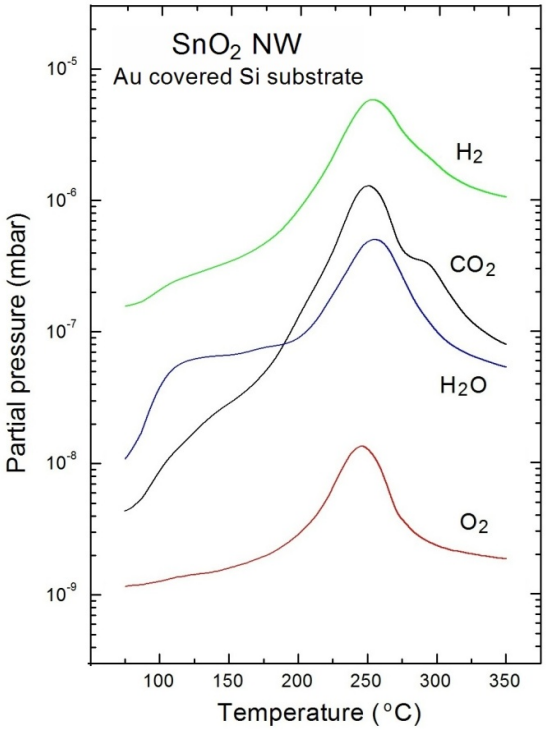

Figure 5. TDS spectra of main residual gases desorbed from the VPD SnO_2 nanowires deposited on Au-covered Si substrate.

One can easily note that the molecular oxygen (O_2) desorbs from VPD SnO_2 nanowires at the partial pressure of about 10^{-8} mbar at 240°C (maximum of the mass peak at this temperature). It means that the oxygen is probably only partially bounded to Sn creating the SnO_2 forms, and that there is a small amount of residual oxygen, which is physically bounded to the surface of VPD SnO_2 nanowires, that can easily desorb during TDS experiment. This conclusion from the TDS spectra corresponds to a decrease of [O]/[Sn] concentration after thermal desorption, as it was shown in XPS measurements.

In turn, molecular hydrogen desorbs during the TPD process at the highest partial pressure of 10^{-5} mbar, with a maximum at 240°C. This last observation is also probably related to the single crystalline form of SnO_2 nanowires [28], like in previously analysed VPD SnO_2 nanowires. This is because molecular hydrogen exhibits the tendency to deeply penetrate the subsurface crystalline region [29], and in this case also inside Au clusters, combined with the fast and strong desorption during TDS experiments.

For the case of water vapour (H_2O), the maximum partial pressure was observed at 10^{-6} mbar, at about 260°C. What is even more important, the fastest desorption of H_2O is seen at the temperature close to 100°C.

The most important TPD effect was observed for carbon dioxide (CO_2). The respective TDS spectrum exhibits a more complicated asymmetric and not-regular shape in the temperatures range 250÷320°C. It probably means that C containing surface contaminations is bounded in two different forms, and with different bonding energies at the external surface of crystalline VPD SnO_2 nanowires.

Peer-reviewed version available at Nanomaterials 2018, 8, 738; doi:10.3390/nano8090738

These last observations related to the desorption behaviour of O_2 and H_2O are in a good correlation with the decrease of the relative [O]/[Sn] concentration observed by XPS (see Fig.3, Table 3.). In turn, the desorption behaviour of CO_2 explains the removal of C contaminations from these VPD SnO_2 nanowires (see XPS C1s spectra in Fig 2.).

The information presented above on the surface non-stoichiometry and surface C contaminations of VPD SnO_2 nanowires is extremely important because of two reasons:

(1) The evident surface non-stoichiometry observed for VPD SnO_2 nanowires causes their improved gas sensitivity, especially for oxidizing gases, with respect to the commonly used two-dimensional (2D) nanostructures [16].

(2) The existence of surface C contaminations at the surface, observed even after TDS process, can play an undesired role acting as a specific barrier for the gas adsorption during the gas sensing process, and causing, among others, longer response and recovery times. This may be an evident limitation of their potential application for gas sensors systems.

5. Conclusions

The comparative investigation of VPD SnO_2 nanowires deposited on Au-covered Si substrate using XPS, TDS and SEM methods showed that:

1) SnO_2 nanowires exhibit a slight deviation from stoichiometry both before and after TDS. However, the presence of oxygen vacancy defects can lead to the improved gas sensitivity especially for oxidizing gases.

2) Carbon contamination appears on the surface of SnO_2 nanostructures. Its contribution decreases after TDS procedure, however it cannot be completely removed, unlike in the corresponding experiments performed on Ag-assisted SnO_2 nanowires.

3) Au metallic particles present on the surface of nanowires impede carbon desorption during TDS.

4) All other active gases, physically adsorbed at the surface of VPD SnO_2 nanowires after atmosphere exposure and creating surface contaminations, are almost fully desorbed during TDS.

5) Based on the results of deconvolution procedure, it can be concluded that the surface chemistry of VPD SnO_2 nanowires is stable.

Acknowledgments: This work was realized within the Statutory Funding of Institute of Electronics, Silesian University of Technology, Gliwice, BK - 2017 as well as BKM-510/RAu3/2017, as well as partially supported by the research grant of National Science Centre, Poland grant decision DEC-2016/20/S/ST5/00165.

Author Contributions: M.K. involved in carrying out the XPS and TDS experiments, analyzing the experimental data and drafting he manuscript; B.L.-S. conceived the XPS, conducted data analysis, and verified the manuscript. A.K. carried out the TDS measurements, V.G. involved in the preparation of samples and SEM experiments with data analysis; E.C.. conceived of the study. All authors read and approved the final version of the manuscript.

Conflicts of Interest: The authors declare no conflict of interest.

References

1. Göpel, W.; Schierbaum, K.D. SnO_2 sensors: current status and future prospects, *Sens. Actuators B Chem. 26,* **1995**, 1 – 12, DOI: 10.1016/0925-4005(94)01546-T.
2. Lewis, B.G.; Paine, D.C. Applications and processing of transparent conducting oxides, *MRS Bull. 25,* **2000**, 22 – 27, DOI: 10.1557/mrs2000.147.

3. Hartnagel, H.L.; Dewar, A.L.; Jain, A.K.; Jagadish, C. Semiconducting transparent thin films, *IOP Publishing*, Bristol **1995,** ISBN 9780750303224.
4. Park, S.; Zheng, H.; Mackenzie, J.D. Sol-gel derived antimony-doped tin oxide coatings on ceramic cloths, *Mater. Lett. 22*, **1995**, 175 – 180, DOI: 10.1016/0167-577X(94)00241-X.
5. Khan, A.; Mehmood, M.; Aslam, M.; Ashraf, M. Characteristics of electron beam evaporated nanocrystalline SnO_2 thin films annealed in air, *Appl. Surf. Sci. 256*, **2010**, 2252 – 2258, DOI: 10.1016/j.apsusc.2009.10.047.
6. Hübner, M.; Koziej, D.; Grunwaldt, J.-D.; Weimar, U.; Barsan, N. An Au clusters related spill-over sensitization mechanism in SnO_2-based gas sensors identified by operando HERFD-XAS, work function changes, DC resistance and catalytic conversion studies, *Phys. Chem. Chem. Phys. 14*, **2012**, 13249 – 13254, DOI: 10.1039/C2CP41349C.
7. Barsan, N.; Hübner, M.; Weimar, U. Conduction mechanism in SnO_2 based polycrystalline thick film gas sensors exposed to CO and H_2 in different oxygen background, *Sens. Actuators B Chem. 157*, **2011**, 510 – 517, DOI: 10.1016/j.snb.2011.05.011.
8. Yamazoe, N.; Shimanoe, K. Oxide semiconductor gas sensors, *Catal. Surv. Asia 7(1)*, **2003**, 63 – 75, DOI: 10.1023/A:1023436725457.
9. Sitarz, M.; Kwoka, M.; Zappa, D.; Comini, E.; Szuber, J. Surface chemistry of SnO_2 nanowires on Ag – catalyst – covered Si substrate studied using XPS and TDS methods, *Nanoscale Res. Lett. 9*, **2014**, 43 – 48, DOI: 10.1186/1556-276X-9-43.
10. Luo, S.; Fan, J.; Liu, W.; Zhang, M.; Song, Z.; Lin, C.; Wu, X.; Chu, P. Synthesis and low-temperature photoluminescence properties of SnO_2 nanowires and nanobelts, *Nanotechnology 17*, **2006**, 1695 – 1699, DOI: 10.1088/0957-4484/17/6/025.
11. Katoch, A.; Sun, G.-J.; Choi, S.-W.; Hishita, S.; Kulish, V.V.; Wu, P.; Kim, S. Acceptor – compensated charge transport and surface chemical reactions in Au – implanted SnO_2 nanowires, *Sci. Rep. 4*, **2014**, 4622 – 4629, DOI: 10.1038/srep04622.
12. Park, J.Y.; Asokan, K.; Choi, S.-W.; Kim, S.S. Growth kinetics of nanograins in SnO_2 fibers and size dependent sensing properties, *Sens. Actuators B Chem. 152*, **2011**, 254 – 260, DOI: 10.1016/j.snb.2010.12.017.
13. Lyson – Sypien, B.; Czapla, A.; Lubecka, M.; Kusior, E.; Zakrzewska, K.; Radecka, M.; Kusior, A.; Balogh, A.G.; Lauterbach, S.; Kleebe, H.-J. Gas sensing properties of TiO_2-SnO_2 nanomaterials, *Sens. Actuators B Chem. 187*, **2013**, 445 – 454, DOI: 10.1016/j.snb.2013.01.047.
14. Choi, S.-W.; Katoch, A.; Sun, G.-J.; Wu, P.; Kim, S.S. NO_2 – sensing performance of SnO_2 microrods by functionalization of Ag nanoparticles, *J. Mater. Chem. C 1*, **2013**, 2834 – 2841, DOI: 10.1039/C3TC00602F.
15. Comini, E. Metal oxide nano - crystals for gas sensing, *Anal. Chim. Acta 568*, **2006**, 28–40, DOI: 10.1016/j.aca.2005.10.069.
16. Kolmakov, A.; Moskovits, M. Chemical sensing and catalysis by one – dimensional metal oxide nanostructures, *Annu. Rev. Mater. Res. 34*, **2004**, 151 – 180, DOI: 10.1146/annurev.matsci.34.040203.112141.
17. Yamazoe, N.; Shimanoe, K. Basic approach to the transducer function of oxide semiconductor gas sensors, *Sens. Actuators B Chem. 160*, **2011**, 1352 – 1362, DOI: 10.1016/j.snb.2011.09.075.
18. Kolmakov, A.; Klenov, D.O.; Lilach, Y.; Stemmer, S.; Moskovits, M. Enhanced gas sensing by individual SnO_2 nanowires and nanobelts functionalized with Pd catalyst particles, *Nano Lett. 5(4)*, **2005**, 667 – 673, DOI: 10.1021/nl050082v.
19. Shen, Y.; Yamazaki, T.; Liu, Z.F.; Meng, D.; Kikuta, T.; Nakatani, N.; Saito, M.; Mori, M. Microstructure and H_2 gas sensing properties of undoped and Pd-doped SnO_2 nanowires, *Sens. Actuators B Chem. 135*, **2009**, 524 – 529, DOI: 10.1016/j.snb.2008.09.010.

20. Choi, S.-W.; Katoch, A.; Sun, G.-J.; Kim, S.S. Bimetallic Pd/Pt nanoparticle-functionalized SnO_2 nanowires for fast response and recovery to NO_2, *Sens. Actuators B Chem. 181*, **2013**, 446 – 453, DOI: 10.1016/j.snb.2013.02.007.
21. Shafiei, M.; Kalantar-Zadeh, K.; Wlodarski, W.; Comini, E.; Ferroni, M.; Sberveglieri, G.; Kaciulis, S.; Pandolfi, L. Hydrogen gas sensing performance of Pt/SnO_2 nanowires/SiC MOS devices, Int. *J. Smart Sensing Intell. Syst. 1*, **2008**, 771 – 783, DOI: 10.21307/ijssis-2017-319.
22. Hwang, I.-S.; Choi, J.-K.; Woo, H.-S.; Kim, S.-J.; Jung, S.-Y.; Seong, T.-Y.; Kim, I.-D.; Lee, J.-H. Facile control of C_2H_5OH sensing characteristics by decorating discrete Ag nanoclusters on SnO_2 nonowire networks, *ACS Appl. Mater. Interfaces 3*, **2011**, 3140 – 3145, DOI: 10.1021/am200647f.
23. Yin, W.; Wei, B.; Hu, C. In situ growth of SnO_2 nanowires on the surface of Au – coated Sn grains using water – assisted chemical vapor deposition, *Chem. Phys. Letters 471*, **2009**, 11 – 16, DOI: 10.1016/j.cplett.2009.02.021.
24. Xia, Y.; Yang, P.; Sun, Y.; Wu, Y.; Mayers, B.; Gates, B.; Yin, Y.; Kim, F.; Yan, H.One-dimensional nanostructures: synthesis, characterization and applications, *Adv. Mater. 15*, **2003**, 353 – 389, DOI: 10.1002/adma.200390087.
25. Sberveglieri, G.; Baratto, C.; Comini, E.; Faglia, G.; Ferroni, M.; Pardo, M.; Ponzoni, A.; Vomiero, A. Semiconducting tin oxide nanowires and thin films for chemical warfare agents detection, *Thin Solid Films 517*, **2009**, 6156 – 6160, DOI: 10.1016/j.tsf.2009.04.004.
26. Wagner, C.D.; Riggs, W.M.; Davis, L.E.; Moulder, J.F.; Mnilenberger, G.E. Handbook of Xray Photoelectron Spectroscopy, *Perkin-Elmer*, Eden Prairie, MN, **1979**, ISBN 9780962702624.
27. NIST X-ray Photoelectron Spectroscopy Database. Available online: http://srdata.nist.gov/xps/ (accessed on 22.03.2018)
28. Comini, E.; Baratto, C.; Faglia, G.; Ferroni, M.; Vomiero, A.; Sberveglieri, G. Quasi-one dimensional metal oxide semiconductors: Preparation, characterization and application as chemical sensors, *Prog. Mater. Sci. 54*, **2009**, 1 – 67, DOI: 10.1016/j.pmatsci.2008.06.003.
29. Comini, E.; Faglia, G.; Ferroni, M.; Ponzoni, A.; Vomiero, A.; Sberveglieri, G. Metal oxide nanowires: Preparation and application in gas sensing, *J. Molec. Catal. A: Chem. 305*, **2009**, 170 – 177, DOI: 10.1016/j.molcata.2009.01.009.